arXiv:1108.4186v1 [cond-mat.str-el] 21 Aug 2011

Complex magnetism and magnetic field-driven electrical polarization in Co_3TeO_6

M. Hudl,[1,*] R. Mathieu,[1] S. A. Ivanov,[1,2] M. Weil,[3] V. Carolus,[4] Th. Lottermoser,[4,5] M. Fiebig,[4,5] Y. Tokunaga,[6] Y. Taguchi,[7] Y. Tokura,[6,7,8] and P. Nordblad[1]

[1] *Department of Engineering Sciences, Uppsala University, Box 534, SE-751 21 Uppsala, Sweden*
[2] *Department of Inorganic Materials, Karpov' Institute of Physical Chemistry, Vorontsovo pole, 10 105064, Moscow K-64, Russia*
[3] *Institute for Chemical Technologies and Analytics, Vienna University of Technology, A-1060 Vienna, Austria*
[4] *HISKP, Universität Bonn, Nussallee 14-16, 53115 Bonn, Germany*
[5] *Department of Materials, ETH Zurich, 8093 Zurich, Switzerland*
[6] *Multiferroics Project, ERATO, Japan Science and Technology Agency (JST), Wako 351-0198, Japan*
[7] *Cross-Correlated Materials Research Group (CMRG) and Correlated Electron Research Group (CERG), ASI, RIKEN, 2-1 Hirosawa, Wako 351-0198, Japan*
[8] *Department of Applied Physics, University of Tokyo, Tokyo 113-8656, Japan*

(Dated: August 23, 2011)

The magnetic and electrical properties of Co_3TeO_6 single-crystals with corundum related structure reveal a magnetic-field induced polarization below 21 K. A sharp peak in the specific heat at ≈18 K indicates a reconstructive-type first-order phase transition. From second-harmonic generation (SHG) measurements breaking of inversion symmetry is evident and the point-group symmetry was determined as m. The temperature and magnetic-field dependence of the magnetic and electrical polarizations are discussed in the light of the SHG results.

PACS numbers: 75.47.Lx, 75.85.+t, 75.50.Ee

Tailoring materials with coupled magnetic and electrical properties is a challenge in condensed-matter science [1–3]. For example in a magnetoelectric multiferroic material, the electrical polarization may be controlled by a magnetic field instead of its natural stimuli, an electric field, and vice versa [4, 5]. In contemporary studies of what is called joint-order-parameter (type II) multiferroics this coupling can be achieved by a variety of mechanisms coupling an improper electric polarization to the magnetic order, e.g., via symmetric or antisymmetric exchange interactions or a spin-dependent d-p hybridization. For example, the antisymmetric Dzyaloshinskii-Moriya interaction can induce an electric polarization according to $P \propto \sum e_{ij} \times (s_i \times s_j)$ where e_{ij} is the vector connecting the two neighboring spins s_i and s_j [6, 7]. Even though exhibiting a rather small spontaneous electrical polarization the coupling of magnetic and electrical properties in these materials is inherently stronger than that of split-order-parameter (type-I) multiferroics, where magnetic and ferroelectric order emerge independently [8]. New magnetoelectric multiferroics are thus to be found among materials with magnetic structures dominated by frustration and competing interactions. In this context, it is interesting to investigate physical properties of the sparsely characterized corundum-related M_3TeO_6 compounds, where M is a first-row transition metal. Ni_3TeO_6 was found to order antiferromagnetically below 52 K, with a relatively simple magnetic structure [9]. Mn_3TeO_6 on the other hand was recently reported to exhibit a complex incommensurate spin structure, consisting of two different magnetic orbits [10]. The magnetic and electrical properties of Co_3TeO_6 are unknown to date, although its structure shows some interesting features which may strongly influence its magnetic ordering. There are five distinguishable sites for the magnetic Co^{2+} cations and the <Co-O> bond length varies greatly from 1.97 to 2.93 Å.

In this communication we report the first results on the magnetic and electrical properties of Co_3TeO_6 single-crystals. The evolution of the magnetization and polarization of Co_3TeO_6 with temperature and magnetic field suggests a complex magnetic structure as well as spin rearrangements and spin-flop transitions. The magnetic structure of the compound promotes a magnetic-field induced polarization below 21 K. The origin and nature of the polarization is discussed in the light of optical second-harmonic generation (SHG) data indicating magnetically broken inversion symmetry.

High-quality single crystals of Co_3TeO_6 were grown by chemical transport reactions [11]. A mixture of CoO and TeO_3 (obtained by heat treatment of $Co(NO_3)_2{\cdot}6H_2O$ and H_6TeO_6 respectively) in the stoichiometric ratio 3:1 was thoroughly ground and was, together with 10 mg $PtCl_2$, placed in a silica ampoule which was evacuated, sealed, and heated in a temperature gradient 1098 → 1028 K. After 5 days the transport reaction was completed and dark blue to black crystals of Co_3TeO_6, mostly with a prismatic pinacoidal form and edge-lengths up to 5 mm, had formed in the colder part of the ampoule. X-ray powder diffraction patterns were recorded on crushed single crystals using a Bruker D-8 diffractometer with CuKα radiation, and analyzed with Rietveld techniques using FULLPROF software.

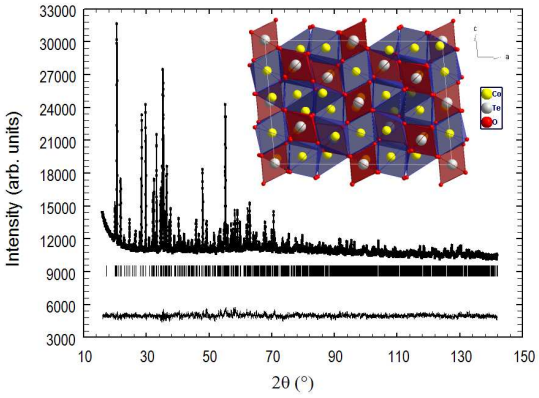

FIG. 1. (Color Online) X-ray diffraction pattern and Rietveld refinement for Co_3TeO_6 at room temperature (Rietveld residuals: $R_p = 2.07\%$, $R_{wp} = 3.49\%$, $R_b = 6.42\%$. See Ref. [12] for details; the Rietveld analysis confirmed the absence of impurity phases). Inset presents an polyhedral representation of the structure.

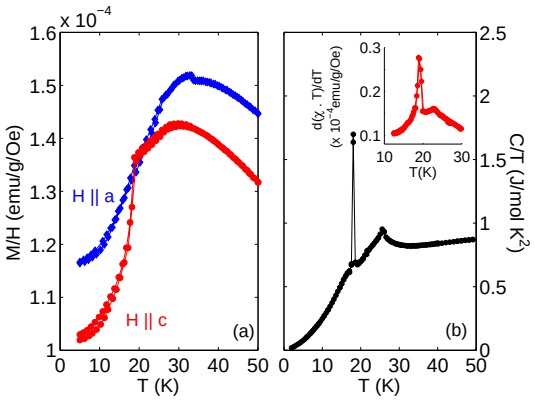

FIG. 2. (Color online) Temperature dependence of (a) the zero-field cooled (ZFC) and field-cooled (FC) magnetization in 20 Oe magnetic field for different orientations, and (b) heat capacity, plotted as C/T. No significant differences were observed in heat capacity measurements recorded on cooling and heating [16]. The inset shows the temperature dependence of $d\chi T/dT$ ($\chi = M/H$) calculated from the magnetization data with $H||c$.

Magnetization measurements up to 20 Oe were performed using a Quantum Design MPMS XL SQUID magnetometer following zero-field-cooled (ZFC) and field-cooled (FC) protocols, while magnetization measurements above 20 Oe (using a VSM), heat capacity (using a relaxation method) as well as pyroelectric measurements were performed on a Quantum Design PPMS. In order to check the magnetoelectric response; thin plates of Co_3TeO_6 crystals, oriented perpendicular to the a-axis [13] and the c-axis respectively, were prepared. In the experiments, these were poled in a ≈ 500 V/mm electric field and cooled from 50 K in the PPMS. The electrical polarization P was obtained from integrating the pyroelectric current recorded using an electrometer (Keithley 6517A). For nonlinear optical experiments [14] crystals were polished to about 50 μm thickness with orientations perpendicular to the crystallographic a, b and c axis, respectively. The samples were mounted in a He-vapor-operated cryostat and excited by light pulses (5 ns, 10-40 Hz, 2.3-2.9 eV) generated with an optical parametric oscillator pumped by a Nd:YAG laser. Signals were detected by a liquid-nitrogen-cooled digital camera.

The X-ray diffraction pattern and associated Rietveld refinement at 296 K is shown in Fig. 1. Co_3TeO_6 adopts a monoclinic structure (space group $C2/c$), with lattice parameters $a = 14.8014(3)$Å, $b = 8.8379(2)$Å, $c = 10.3421(3)$Å, and monoclinic angle $\beta = 94.83(1)$. These values are in good agreement with those of the previous single crystal study [15]. There are five distinguishable Co^{2+} sites, out of which three are octahedrally, one is square-pyramidally and one is tetrahedrally coordinated. The two distinct Te^{6+} sites have an octahedral coordination [15].

Low-magnetic field (20 Oe) ZFC and FC magnetization data of Co_3TeO_6 for different orientations of the applied magnetic field H are shown in Fig. 2(a). The magnetization recorded with H applied along the a-axis and the c-axis exhibits a maximum close to 30 K suggesting antiferromagnetic ordering. In both cases a marginal irreversibility between the ZFC/FC curves is observed at low temperature. For the magnetization recorded with $H||a$ a small but distinct step of unknown nature is observed in both the ZFC and FC curves just above 30 K. With $H||c$, a sharp drop in the magnetization is observed at T* $\sim$ 18 K. A Curie-Weiss analysis of the high-temperature magnetization data was performed, yielding a Weiss constant of $\theta = -54$ K and an effective Bohr magneton number of $p = 4.69$. The θ and p values confirm an (antiferro)magnetic interaction and covalency effects, respectively [17]. The heat-capacity data shown in Fig. 2(b) confirms that a long-range (antiferromagnetic) order is established near 26 K. Interestingly, a sharp peak is observed at 18 K, i.e. in the vicinity of T*. Such a δ-peak-like anomaly in the heat capacity could be an indication for a reconstructive first-order phase transition [18]. Both features at 26 K and 18 K are evident in the temperature derivative of the magnetic susceptibility ($\chi = M/H$) times temperature (T), $d(\chi \cdot T)/dT$, as seen in inset of Fig. 2(b). ($(d(\chi \cdot T)/dT)$ should be proportional to the magnetic specific heat for an antiferromagnet [19]). Neutron powder diffraction experiments on crushed single crystals suggest a magnetic structure involving several propagation vectors [12].

The symmetry properties of long-range ordered and, in particular, non-centrosymmetric compounds can be probed by SHG. In the electric-dipole approximation

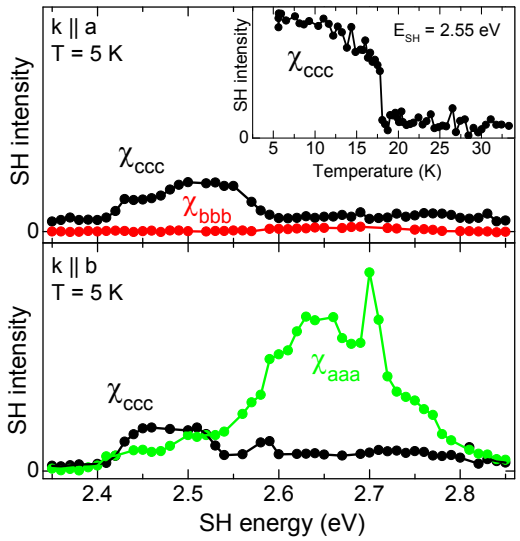

FIG. 3. (Color online) Second harmonic generation at 5 K for $k \parallel a$ (upper panel) and $k \parallel b$ (lower panel). k represents the wave vector of the incident light and χ_{aaa} and χ_{ccc} are SHG susceptibility tensor components; the red line depicts χ_{bbb} which does not contribute to the SHG signal. The inset shows the temperature dependence of χ_{ccc}.

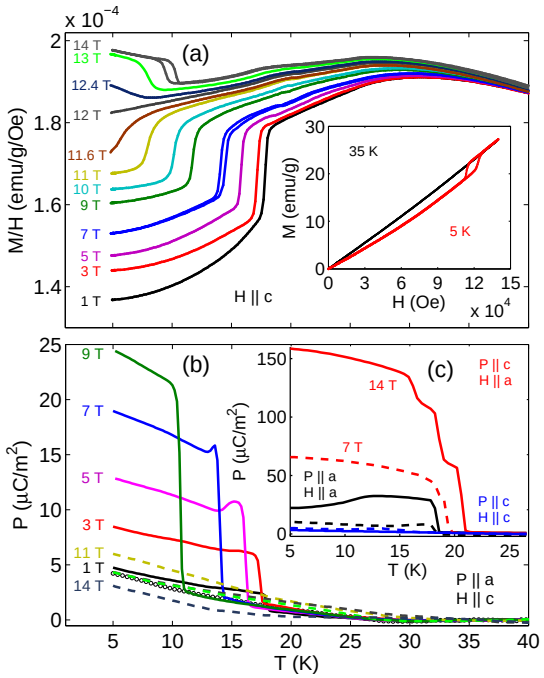

FIG. 4. (Color online) (a) Field-cooled magnetization and (b) electric polarization as a function of temperature in several magnetic fields up to 14 T applied along the c-axis. The magnetization curves for 7 T and 14 T field are shown for both cooling and heating sweeps. Inset in (a) shows magnetization as a function of magnetic field at 5 K and 35 K. In (c) the temperature dependence of the polarization for applied magnetic fields of 7 T and 14 T for different orientations of the applied magnetic field and measured polarization is presented.

SHG can be described by $P_i(2\omega) = \epsilon_0\, \chi_{ijk}\, E_j(\omega)\, E_k(\omega)$, where $\vec{E}(\omega)$ and $\vec{P}(2\omega)$ represent the incident light at frequency ω and the polarization induced at frequency 2ω [14]. The set of nonzero tensor components χ_{ijk} is determined by the symmetry of the material. In the case of inversion symmetry we have $\chi_{ijk} \equiv 0$. Therefore one would not expect any SHG signal for Co_3TeO_6 in the non-ferroic phase above T_N with the space group $C2/c$ (point group $2/m$). A broken inversion symmetry in the low temperature ferroic phase would reduce the point symmetry to m, 2 or 1, respectively [20] and induce nonzero components according to: m (χ_{aaa}, χ_{ccc}), 2 (χ_{bbb}), 1 (χ_{aaa}, χ_{bbb}, χ_{ccc}). As shown in Fig. 3 there are χ_{aaa} and χ_{ccc} contributions to the SHG in the a and b cut samples in the low temperature phase, but no signal for the χ_{bbb} component. This reveals m as the point symmetry for this phase. For point-group symmetry m a polar axis in the ac-plane perpendicular to the monoclinic b-axis exist [20]. This means a possible ferroelectric polarization would be oriented parallel to this polar axis. Furthermore, in the inset of Fig. 3, the ferroic transition at 18 K is evidenced from the temperature dependence of χ_{ccc}. Notwithstanding that our SHG data indicate magnetically broken inversion symmetry a possible absence of the spontaneous polarization needs to be considered.

Magnetic and electrical properties in high-magnetic fields up to 14 Tesla are depicted in Fig. 4. The FC cooling magnetization measurements in c-axis orientation reveal that the drop in magnetization (observed at 18 K in low-fields) is shifted towards lower temperatures with increasing applied magnetic fields. For magnetic fields larger than 11 T an upward step is observed in the magnetization data instead of a drop. The rearrangement of the magnetization at low temperatures can also be perceived in magnetization vs. magnetic field measurements, such as the ones shown in the inset of Fig. 4(a).

At 5 K, a possible spontaneous polarization of the order 5 μC/m^2 (close to the resolution limit of our experimental set-up) was measured, see Fig. 4(b) (open data markers).When applying magnetic fields relatively large polarization values are induced below 21 K. As can be seen in Fig. 4(b), the magnetic-field induced polarization ($P||a$, $H||c$) reaches a value of about 25 μC/m^2 at 5 K and 9 T. When the magnetic field is increased beyond 9.3 T the electrical polarization gets rapidly suppressed. The temperature dependence of the magnetic-field induced polarization at 7 T and 14 T field recorded for different orientations of the applied magnetic field and measured polarization is depicted in Fig. 4(c). For orientation ($P||c$, $H||a$) the polarization steadily increases with increasing magnetic field, and reaches about 160 μC/m^2 in 14 T. The electric polarization is strongly interconnected with magnetic

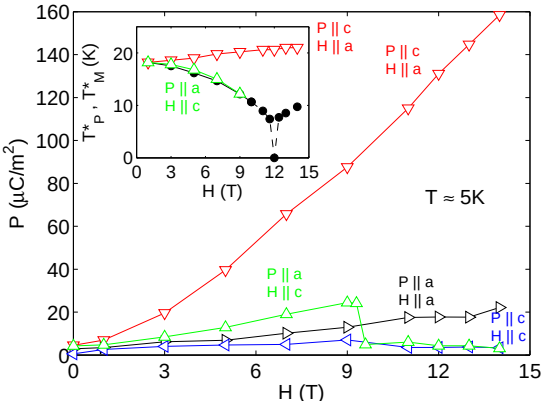

FIG. 5. (Color online) Low-temperature polarization as a function of magnetic field for the different P and H orientations considered. The inset shows the variation of the temperature onset of polarization T_P^* for ($P||c$, $H||a$) (▽) and ($P||a$, $H||c$) (△), as well as the temperature T_M^* (•) below which a drop/step is observed in the magnetization recorded with $H||c$.

behavior, as illustrated in the inset of Fig. 5. The onset of the field-induced polarization ($P||a$, $H||c$) occurs at the same temperatures as the drop (or step) in the magnetization T_M^*. Furthermore, the temperature onset of the induced polarization T_P^* has an orientational dependence on the magnetic field, as seen in the same inset. For $H||a$ the temperature onset of polarization increases with increasing magnetic field whereas for $H||c$ the polarization onset decreases.

Two characteristic temperatures were observed in the low-field magnetization, polarization, heat capacity and neutron data [12], T_N (∼26 K) and T* (∼18 K). At T_N, the spins may form a sinusoidal antiferromagnetic arrangement directed along the c-axis which turns into a spin spiral arrangement below T*. According to SHG, the point symmetry of the low-temperature phase is m, suggesting that the orientation of a possible electrical polarization would be in the "ac"-plane [20]. In view of the present data it is difficult to identify the mechanism for the magnetic-field induced polarization in Co_3TeO_6. However, considering several characteristic features, such as: an incommensurate magnetic structure, a relatively large field-orientation dependence of the induced polarization, and a relatively small value of induced polarization; symmetric exchange striction should not be relevant. On the other hand, from the H-dependence of P shown in Fig. 5, the low-temperature polarization both along a and c increases as $H||a$ is increased. In case of a spiral magnetic structure, it may be difficult to attribute these observations to an antisymmetric exchange mechanism alone, while a gradual rotation of the spiral plane and the subsequent increase of the cycloidal components may explain the H-dependence of the polarization in the case of $P||c$.

To conclude, we have investigated the magnetic, electrical, specific heat, and non-linear optical properties of Co_3TeO_6 single-crystals. Specific heat data reveal (antiferro)magnetic ordering at ∼26 K and a first-order-like phase transition at ∼18 K, both likewise observed in the magnetic measurements. The magnetic structure brings forth a magnetic-field induced electrical polarization. For magnetic fields $H||c$ the induced polarization is suppressed above 9.3 T whereas for $H||a$ a significant enhancement of $P||c$ up to 160 μC/m^2 is observed in 14 T. Our results suggest a strong coupling for the magnetic and electrical structure of Co_3TeO_6 below 21 K. We therefore believe that corundum-related compounds such as Co_3TeO_6 are a new interesting class of magnetoelectric multiferroic systems.

We thank P. Tolédano for discussions. We acknowledge and thank the Swedish Research Council (VR), the Göran Gustafsson Foundation, Anna-Maria Lundin foundation, Hans Werthén Fonden, the FIRST Program by JSPS, SFB608 of the DFG, and the Russian Foundation for Basic Research for financial support.

* matthias.hudl@angstrom.uu.se

[1] T. Kimura, T. Goto, H. Shintani, K. Ishizaka, T. Arima, and Y. Tokura, Nature **426**, 55 (2003).
[2] H. Hur, S. Park, P. A. Sharma, J. S. Ahn, S. Guha, and S.-W. Cheong, Nature **429**, 392 (2004).
[3] N. A. Spaldin and M. Fiebig, Science **309**, 391 (2005); N. A. Hill, J. Phys. Chem. B **104**, 6694 (2000); M. Fiebig, J. Phys. D **38**, R123 (2005).
[4] Th. Lottermoser, T. Lonkai, U. Amann, D. Hohlwein, J. Ihringer, and M. Fiebig, Nature **430**, 541 (2004).
[5] M. Gajek, M. Bibes, S. Fusil, K. Bouzehouane, J. Fontcuberta, A. Barthelemy, and A. Fert, Nature Mater. **6**, 296 (2007).
[6] H. Katsura, N. Nagaosa, and A. V. Balatsky, Phys. Rev. Lett. **95**, 057205 (2005).
[7] K. V. Shanavas, D. Choudhury, I. Dasgupta, S. M. Sharma, and D. D. Sarma, Phys. Rev. B **81**, 212406 (2010).
[8] D. Khomskii, Physics **2**, 20 (2009); S.-W. Cheong and M. Mostovoy, Nature Mater. **6**, 13 (2007).
[9] I. Zivkovic, K. Prsa, O. Zaharko, and H. Berger, J. Phys.: Condens. Matter **22**, 056002 (2010).
[10] S. A. Ivanov, P. Nordblad, R. Mathieu, R. Tellgren, C. Ritter, N. Golubko, E. D. Politova, and M. Weil, to appear in Mater. Res. Bull. (2011); cond-mat/1104.5560.
[11] H. Schäfer, *Chemical Transport Reactions* (Academic Press - New York, 1963).
[12] S. A. Ivanov et al., unpublished.
[13] The a-axis sample for the electrical polarization measurements may involve a b-axis component such as [310].
[14] M. Fiebig, V. V. Pavlov, and R. V. Pisarev, J. Opt. Soc. Am. B **22**, 96 (2005).
[15] R. Becker, M. Johnsson, and H. Berger, Acta Cryst. **C62**, i67 (2006).

[16] R. Nirmala, D. Paudyal, V. K. Pecharsky, K. A. Gschneidner Jr., and A. K. Nigam, J. Appl. Phys. **109**, 07A923 (2011).
[17] R. Mathieu, S. A. Ivanov, R. Tellgren, and P. Nordblad, Phys. Rev. B **83**, 174420 (2011).
[18] P. Tolédano and V. Dmitriev, *Reconstructive phase transition: in crystals and quasicrystals* (World Scientific Publishing, Singapore, 1996).
[19] M. E. Fisher, Phil. Mag.) **7**, 1731 (1962); P. Nordblad, L. Lundgren, E. Figueroa, and O. Beckman, J. Magn. Magn. Mater. **23**, 333 (1981).
[20] R. R. Birss, *Symmetry and magnetism* (North-Holland Publishing Company, Amsterdam, 1966).